

# Optimization of the Solar Energy Collection in Tracking and Non-Tracking Photovoltaic Solar System

Pavel Yu. Vorobiev  
Facultad de Ingeniería  
Universidad Autónoma de Queretaro  
C.P. 76010, Queretaro, Qro., MEXICO

Jesús González-Hernández, Yuri V. Vorobiev  
Unidad Queretaro of CINVESTAV  
CINVESTAV-IPN  
Queretaro-76230, QRO., MEXICO

**Abstract** – Experimental and theoretical analysis is made of the conditions of collection of solar radiation in solar tracking system without concentration, and in non-tracking system with standard and bifacial photovoltaic solar panel. For the experiments with solar tracking, an original Sun tracker was developed. The tracking effect calculated and measured shows an increase in energy collection around 30 – 40 %; bifacial panels with a reflector collecting solar radiation for the rear face give the corresponding increase of 50 – 60 % for the same panel area.

## 1. INTRODUCTION

The efficiency of solar energy conversion by photovoltaic (PV) panels is the problem which constantly is in a focus of attention of scientists and technologists in the field. One of its many aspects is the concentration of solar radiation and/or tracking of the Sun, to increase the total energy collected by a panel for conversion. Significant progress achieved here during the last decade was mainly due to employment of semiconductor high technology and high degree of concentration. The purpose of this paper is to analyse the possibilities of increase the efficiency of utilization of solar energy in more practical way, using traditional and bifacial PV panels, low concentration systems and economic Sun trackers.

## II. MODELLING OF DAILY VARIATIONS OF SOLAR RADIATION INTENSITY

To be able to evaluate correctly the amount of solar energy collected by a solar module, one has to know the dependence of solar radiation intensity (i.e. irradiance) for a given module position upon the angle  $\phi$  between the Sun flux direction and zenith. There are many publications on the subject, including different models (for example, [1-6]) which usually demand very detailed information about the state of atmosphere to be used (like light dispersion and absorption caused by water vapor, ozone layer, aerosol, etc.); that makes their utilization for quick estimations practically impossible.

We present here a simple model to calculate the dependence mentioned which is based upon the data known for the solar radiation intensity at different air mass: AM0 (1367W/m<sup>2</sup>), AM1 (925 W/m<sup>2</sup>), AM1.5 (844 W/m<sup>2</sup>) and AM2 (691 W/m<sup>2</sup>); it is generally accepted that the air mass index for the last three values corresponds to  $1/\cos\phi$ , the latter expression is easily associated with an increase of the path of the solar flux in atmosphere with increase of  $\phi$  if one neglect the Earth's curvature (in other words, it is a good approximation for relatively small values of  $\phi$ ; this is one of the points to be analyzed).

To explain the difference between the AM0 value (cosmic intensity F) and those related to the Earth's surface, one has to take into account, except for the losses in passing through atmosphere, also reflection (back scattering, more exactly) from it; this effect in rough approximation could be considered as independent on angle  $\phi$ . Thus, we obtain an approximate dependence of the Sun radiation intensity at the Earth's surface  $I_0$  upon the angle  $\phi$  as follows:

$$I_0 = CF(1 - B/\cos\phi) \quad (1)$$

where the constant C takes account of back scattering, and B is proportional to the atmosphere thickness. It is evident that (1) is an approximate expression valid only for relatively small losses in atmosphere; the better approximation is given by the expression

$$I_0 = CF \exp(-\alpha d) \quad (2)$$

where  $\alpha$  is the effective coefficient of absorption + scattering in the atmosphere, and d – its effective thickness for a given angle (the term "effective" here means that we substitute the real atmosphere with height-dependent parameters by the uniform one having the same total absorption). For  $\alpha d \ll 1$ , we put

$$\exp(-\alpha d) \approx 1 - \alpha d, \quad (2^*)$$

so that  $\alpha d$  in (2) will be equivalent to  $B/\cos\phi$  in (1). If we neglect the Earth's curvature, the effective atmosphere thickness d could be written as  $h/\cos\phi$ , where h is this thickness for zero angle. It means that  $B = \alpha h$ , and (2) could be rewritten as

$$I_0 = AF \exp(-B/\cos\phi) \quad (3)$$

The constants A and B in (1) and (3) we find, averaging the data found from the pairs of algebraic equations obtained by insertion in (1) or (3) the data for AM1 and AM1.5, and then for AM1 and AM2. In case of equation (1) this procedure gives

$$I_0 = 1140(1 - 0.188/\cos\phi) \text{ W/m}^2 \quad (1^*)$$

Using for calculations the equation (3), we get slightly different values of constants:

$$I_0 = 1200 \exp(-0.26/\cos\phi) \text{ W/m}^2 \quad (3^*)$$

The Fig. 1 shows the angular dependencies corresponding to (1\*) and (3\*) as curves 1 (squares) and 2

(circles); it is evident that for angle not exceeding  $60^\circ$ , the curves practically coincide; for larger angles the curve 1 goes down more rapidly, reaching zero value at angle smaller than  $90^\circ$  which is clearly incorrect. Thus, expression (3) is the better approximation here, meaning that the absorption in atmosphere at large angles is not small and the approximation (2\*) is not a good one. We can also note that the curves 1 and 2 in Fig. 1 give for the AM0, AM1.5 and AM2 the values around 925, 840 and  $700 \text{ W/m}^2$  correspondingly, which we consider as good enough approximation.

One can see that the curve 2 in Fig. 1, although gives the larger values at large angles than the curve 1, is also going down to zero at angles smaller than  $90^\circ$ , which clearly could be attributed to the effect of the Earth's curvature: neglecting it, we get the larger atmosphere thickness at large angles than the real one.

To take account of this factor, we have to find the more realistic angular dependence of the effective atmospheric thickness. Fig. 2 gives a sketch of the Earth-atmosphere system, the point O corresponds to the observer's position (solar flux comes from the left, as shown by solid arrows); the values of  $h$  and  $d$  are indicated. Using the theorem stating that at intersection of a chord with a diameter, the products of their parts are equal, we write

$$h \cdot (2R+h) = d \cdot (OL+d), \quad (4)$$

$R$  being the Earth radius.

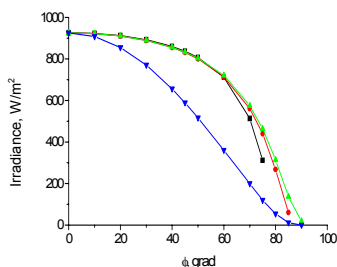


Fig. 1. Angular dependence of direct solar irradiance of a plane surface normal to radiation flux

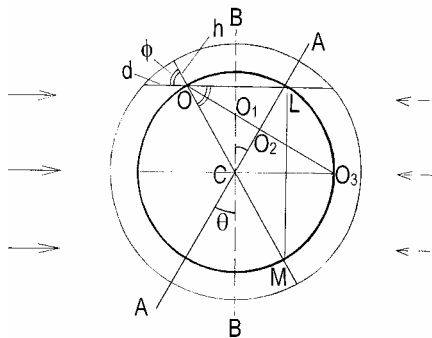


Fig. 2. Scheme of Earth with atmosphere

The triangle OLM is rectangular, so  $OL = 2R \cos\phi$ ; neglecting  $h$  in comparison with  $2R$ , we get from (4)

$$d = R \cos\phi [(1 + 2h/R \cos^2\phi)^{1/2} - 1]. \quad (5)$$

An analysis of the expression obtained shows that for small angles  $\phi$  ( $\cos\phi$  is close to 1, and since  $2h \ll R$ , we can take that  $(1 + 2h/R \cos^2\phi)^{1/2} \approx 1 + h/R \cos^2\phi$ ) the value of  $d$  is approximately equal to  $h/\cos\phi$ , in a good agreement with the discussion above. For angle values close to  $90^\circ$ , (5) gives the finite value  $(2Rh)^{1/2}$ , contrary to the infinity given by  $h/\cos\phi$ .

Having introduced the value of  $d$  given by (5) in the above expression (2) and using, as before, the notation  $B = \alpha h$ , we obtain, instead of (3\*), the new expression

$$I_0 = 1200 \exp\{-0.26R \cos\phi [(1+2h/R \cos^2\phi)^{1/2} - 1]/h\} \text{ W/m}^2 \quad (6)$$

This expression could be considered in our model as the best approximation for the angular dependence of solar radiation. It contains the effective atmospheric thickness  $h$ , but since  $h \ll R$ , for small angles its value is not essential, and for large angles it ought to be found from comparison with the experiment. For initial estimation, we take  $h = 50 \text{ km}$ ; it gave us the curve 3 (triangles) in Fig. 1. It is seen that for angles smaller than  $60^\circ$  this curve practically coincides with curves 1 and 2; for larger angles, curve 3 goes above the other curves, as it should be.

In the following sections we present the calculated and experimental data for the total energy obtained by the panel during the day, for two cases: a) immobile panel, orientated in most profitable manner, and b) the panel with orientation following (tracking) the Sun, i.e. always normal to the radiation flux. The data for the last case ought to be compared with the upper curve in Fig. 1. To be able to discuss the first case, we have drawn the lowest curve in Fig. 1 corresponding to  $I_0 \cos\phi$  where  $I_0$  is given by (6).

### III. EXPERIMENT: RESULTS AND DISCUSSION

#### A. Two-Axis Solar Tracking and its Effect.

The tracking system designed and made uses the solar panel MDSR-65 elaborated by Russian plant OKBKZ, Moscow, has two axis of rotation (Fig. 3). The system is equipped with two geared servo motors (Colman EYQF-33300-661 and Globe 407A-350); 2 pairs of phototransistors (1 pair for each axis) are positioned in such a way that the difference of photoresponce in each pairs is zero when the panel is orientated towards the Sun, and grows with an increase of angle of desorientation. The system monitoring is based on microcontroller PIC16f877 with 4 input channels (one for each sensor); the input analog signals in each channel are digitalized with resolution of 8 bits, the differential signal for each pair is calculated, and the proportional output PWP signal (pulse width modulated) applied to the motors, until the correct position is reached. After that, the system enters the "sleeping state" for the time interval  $X$  which could be chosen depending on the accuracy of tracking necessary.



Fig. 3. Photo of solar tracking system

In our case of a stationary system, the value of  $X = 20$  min was taken, giving the tracking accuracy (i.e. deviation of radiation intensity from maximum) not larger than 0.5 %: the largest corresponding variation of angle  $\phi$  during this interval (at summer time) is 6 grad, and  $\cos 6^\circ = 0.995$ . This tracking system was developed for use with the solar concentrator; the corresponding results will be published separately, here we discuss only the tracking effects without concentration.

To calculate the total solar energy captured daily by the Sun-tracking panel, one needs to change the horizontal axis in Fig. 1 from angle  $\phi$  to corresponding time  $t$ , find the area under the  $I(t)$  curve and double it. For non-tracking panel placed horizontally, the irradiation at arbitrary angle  $\phi$  is proportional to  $\cos\phi$  (the lowest curve in Fig. 1). The ratio of the corresponding areas is 1.354 which means that the calculated tracking effect in the case examined (i.e. that of the vertical Sun orbite) constitutes 35.4 %.

Experimental conditions which correspond to Fig. 1 (i.e. with the maximum at  $\phi = 0$ ) could be realized at summer time, around June 22 (summer solstice), in places of Earth with North latitude close to  $\theta = 23.5^\circ$ , like Guadalajara, Leon or Queretaro in Mexico. Our measurements were made in Queretaro on June 19, 2003, the results are shown in Fig. 4 (triangles with tracking, circles without it). Fig. 2 gives the scheme of experiment: line A-A denotes the Earth rotation axis, Sun flux comes from the right (dashed arrows), the vertical line B-B indicates the boundary between illuminated and dark parts of Earth (day-night),  $O_3$  is the observation point at noon which with time changes its position in relation to Sun following the circular line  $O_3 - O$  (the end of a solar day when  $\phi = 90^\circ$  corresponds to the point  $O_1$ ).

To estimate the duration of a solar day at these conditions, we have to calculate the distance between the points  $O_1$  and  $O_2$  of the circle mentioned; a reasonable approximation could be made on the basis of triangle  $O_1O_2C$ , neglecting the Earth curvature at the corresponding region. Thus we get  $l = O_1O_2 = R \sin\theta \operatorname{tg}\theta$ , and the duration of the day in hours  $t_s = 12 + 24 \cdot 2 \cdot l / 2\pi R \cos\theta = 12 + 24 \operatorname{tg}^2\theta / \pi$ . In the case considered, the day will be 13.44 hrs.

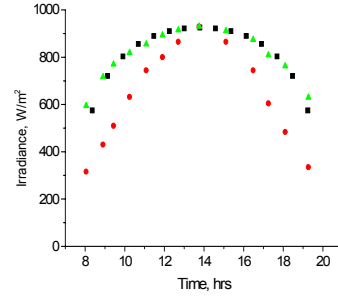


Fig. 4. Experimental and calculated irradiance (see text).

The squares in Fig. 4 show the transformed theoretical upper curve of Fig. 1, adjusted in a way that its maximum coincides with the maximum of experimental curves, the left and right parts are symmetrical in relation to this point, and the angular scale is converted to time so that  $90^\circ$  correspond to 6.72 hrs. One could see that theoretical and experimental data have a reasonable coincidence, although theoretical curve goes a little lower than the experiment at large angles  $\phi$ .

The experimental effect of tracking in our case (i.e. the ratio of areas under the upper and lower curves in Fig. 4) is 1.4, a little higher than the calculated one. The total energy collected by tracking solar module is 6.5 kWh per day per square meter, for non-tracking module it is 4.65 kWh.

For the case of winter insolation at the same latitude (winter solstice, illumination from the left in Fig. 2) our analysis gives the daytime of  $t^* = 12 - 24 \operatorname{tg}^2\theta / \pi = 10.56$  hrs; the maximum irradiance corresponds to the angle of  $47^\circ$  in Fig. 1, and the part of the upper curve between  $47$  and  $90$  grad will describe the time dependence of insolation from noon until the end of the day. The corresponding calculated dependence for the radiation flux captured by the tracking system is shown by squares (the curve starts at irradiance  $825 \text{ W/m}^2$ ) in Fig. 5, where  $\Delta t$  is the time difference from noon.

The lowest curve in Fig. 5 gives the irradiance at winter solstice of non-tracking system orientated in the most favorable way – normal to the solar flux at noon, i.e. at  $47^\circ$  to the Earth surface. During the day, its angle in relation to this flux varies from  $\phi = 0$  to  $\phi = 90^\circ$ , and multiplication of the upper curve by corresponding  $\cos\phi$  gives the irradiance.

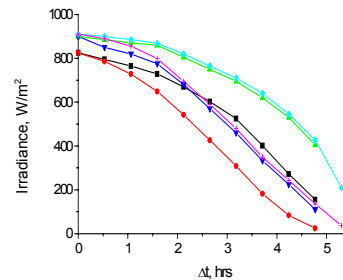


Fig. 5. Irradiance at different periods (see text)

In this case, the calculated tracking effect is 1.28, lower than in summer case. The total energy produced by tracking solar module is 3.6 kWh per day per square meter, for non-tracking module it is 2.8 kWh.

In a similar way, we obtain the irradiance at equinox time, when the smallest value of  $\phi$  at the latitude accepted is  $23.5^\circ$ , and the solar day time is 12 hrs. The calculated data are shown in Fig. 5 by diamonds (the highest curve starting at irradiance  $910 \text{ W/m}^2$ ) for tracking module, and by the curve with crosses starting at the same points for non-tracking one, orientated at  $23.5^\circ$  to the surface and normal to solar flux at noon. Two other curves in Fig. 5 (triangles up and down) are experimental (Queretaro, Mexico, March 20, 2003); they go a little lower than the calculated curves, but reasonably close to them. The experimental tracking effect is 1.33, and the total energy produced by tracking solar module is 4.8 kWh per day per square meter, for non-tracking module it is 3.6 kWh.

### B. Non-Tracking System with Bifacial PV Panel.

We see from the discussion above that the tracking effect in absence of solar concentration is around 30 %, i.e. not very high. There exists another possibility to get more power from PV solar panel of a fixed area – to use bifacial panels [7,8] sensitive to illumination from both sides; usually, the rear face is able to give 50 – 60 % of the power produced by the upper one. These panel demand some arrangements to collect solar radiation for the rear face. One of the approaches [8] is to use the diffuse reflectance from surfaces below the panel, and to paint them correspondingly. This method gives good results; however, it needs relatively large areas of reflecting surfaces, which may be not practical; besides, the paint lasts less than the PV panel. We employed the technique demanding smaller area, which in fact is concentrating reflector placed below the PV panel. Fig. 6 shows a scheme of the reflector, which ideally is a cylindrical or spherical mirror M (the last for a module of approximately squared shape), with a panel (PV) placed in a focal point F, at half a radius from the optical center O.

This reflector with proportions corresponding to our scheme will collect radiation on the rear face of the panel within an angle  $2\theta$  determined by the dimensions of the panel and the reflector focal distance,  $\theta$  gives deviation in position of Sun from zenith.

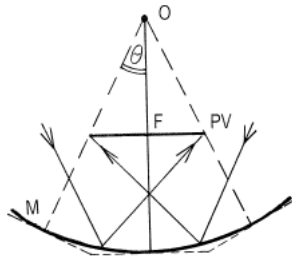


Fig. 6. Optical scheme of reflector for bifacial solar panel



Fig. 7. Two bifacial solar panels with reflectors on the roof of rural school

To make the reflector cheaper, we substituted cylindric surface shown by solid line with plane stainless steel panels as shown by the dashed lines. The actual system with two bifacial panels and reflectors (the other components are not discussed here) was installed in one of the rural schools in the state of Queretaro, Mexico, in August 2002 (Fig. 7), and since then it is constantly used providing enough energy for functioning of the receptor of the satellite educational programs and TV-video set 6 hours a day. Our analysis of the systems performance shows that the panel with efficiency of 10 % and area  $0.6 \text{ m}^2$  having capacity to generate 60 W by front face and 40 W for rear one at AM1.5 illumination conditions, produces 100 W in total, giving 0.6 kWh of electric energy at average summer day, which is better than the data given above for solar tracking panel of the same efficiency.

### IV. CONCLUSIONS

Experimental and theoretical investigations made lead us to the conclusion that the use of solar tracking PV panels in absence of solar concentration gives relatively small increase (around 30 %) in the solar energy collection and electric energy production, and therefore could be practical only with very economic tracking systems. Larger effect could be achieved with bifacial PV panels, which production cost is not much higher than that of standard modules of the same area, and an increase in energy production caused by effective use of a rear face with a simple system of flat mirrors could be 50 – 60 %.

### V. ACKNOWLEDGEMENTS

The authors would like to acknowledge the financial support by CONACYT of Mexico and CONCYTEQ, Queretaro.

## VI. REFERENCES

- [1]. N. Robinson, *Solar Radiation*, Elsevier Publishing, 1971.
- [2]. R.E. Bird, C. Riordan, "Simple Solar Spectral Model for Direct and Diffuse Irradiance", *J. Climate Appl. Meteor.*, vol. 25, 1986, pp. 87-97.
- [3]. J.A. Duffie, W.A. Beckman, *Solar Engineering of Thermal Processes*, 2<sup>nd</sup> ed., Wiley-Interscience, N.Y.; 1991.
- [4]. T.M. Klutcher, "Evaluating Model to Predict Insolation on Tilted Surfaces", *Solar Energy*, vol. 23, 1979, pp. 111-123.
- [5]. V.V. Satyamurty, P.K. Lahiri, "Estimation of Symmetric and Asymmetric Hourly Global and Diffuse Radiation from daily Values", *Solar Energy*, vol. 48, 1992, pp. 7-14.
- [6]. Z.Sen, "Fuzzy Algorithm for Estimation of Solar Irradiation from Sunshine Duration", *Solar Energy*, vol. 68, 1998, pp. 39-49.
- [7]. A. Luque, A. Cuevas, J.M. Ruiz, "Double-sided n<sup>+</sup>-p-n<sup>+</sup> Solar Cell for Bifacial Concentration", *Sol. Cells*, vol. 2, 1980, pp. 151-166.
- [8]. A. Luque, E. Lorenzo and G. Sala, "Diffusing Reflectors for Bifacial Photovoltaic Panels", *Sol. Cells*, vol. 13, 1984-1985, pp. 277-292.